

A novel C-shaped, gold nanoparticle coated, embedded polymer waveguide for localized surface plasmon resonance based detection†

Amit Prabhakar^{ac} and Soumyo Mukherji^{abc}

Received 28th April 2010, Accepted 1st September 2010

DOI: 10.1039/c005253a

In this study, a novel embedded optical waveguide based sensor which utilizes localized surface plasmon resonance of gold nanoparticles coated on a C-shaped polymer waveguide is being reported. The sensor, as designed, can be used as an analysis chip for detection of minor variations in the refractive index of its microenvironment, which makes it suitable for wide scale use as an affinity biosensor. The C-shaped waveguide coupled with microfluidic channel was fabricated by single step patterning of SU8 on an oxidized silicon wafer. The absorbance due to the localized surface plasmon resonance (LSPR) of SU8 waveguide bound gold nano particle (GNP) was found to be linear with refractive index changes between 1.33 and 1.37. A GNP coated C-bent waveguide of 200 μ width with a bend radius of 1 mm gave rise to a sensitivity of $\sim 5 \Delta A/\text{RIU}$ at 530 nm as compared to the $\sim 2.5 \Delta A/\text{RIU}$ (refractive index units) of the same dimension bare C-bend SU8 waveguide. The resolution of the sensor probe was $\sim 2 \times 10^{-4}$ RIU.

1. Introduction

Optical detection techniques used in microfabricated devices are mostly based on optical absorbance or fluorescence detection of analytes,^{1,2} where the detection sensitivity depends on optical density of the analyte, as well as the optical path length in the analyte. Evanescent wave absorbance based schemes are the best solution to these problems but the refractive index sensitivity demonstrated has significant scope for improvement.³ During the last decade, there has been extensive research on localized surface plasmon resonance (LSPR) based biosensors, but there have been relatively few instances of incorporating this in an on chip micro TAS. The phenomenon of localized surface plasmon resonance (LSPR) occurs due to absorption and scattering properties of noble metal nanoparticles, in the UV-visible region.^{4,5} The size, shape and composition of nanoparticles and most significantly the micro-environment around the nanoparticles, have an effect on the extinction band due to LSPR. These properties of noble metal nanoparticles (Au and Ag) have been utilized in the liquid phase as well as in the form of monolayers coated on glass/quartz substrates, using aminosilanes as intermediate layers, to develop colorimetric biosensors.^{6–10} Nano-sphere lithography was used by Van Duyne *et al.*^{11,12} to create Ag nanotriangles on mica substrate and a shift in absorbance peak (λ_{max}) was exploited for biosensing purposes. Chau *et al.*¹³ used GNP coated straight fiber probes for biochemical sensing and Leung *et al.*¹⁴ used GNP coated biconically tapered single mode fiber probes for label free detection

of DNA hybridisation. Recently Sai *et al.*¹⁵ have reported coating of gold nanoparticles on U-bend optical fiber probes for LSPR based biosensors. To the best of our knowledge, no study has been published on combining the advantages of GNP based detection with enhanced evanescent wave absorption, exhibited in bent embedded polymer waveguides. In this article, we report the development of a novel LSPR based lab on a chip device using GNP coated C-shaped SU8 waveguides. We have successfully coupled GNP coated SU8 waveguides with microchannels by a single step patterning of SU8. A complete optical set-up involved a polymer analysis chip probe, a light emitting diode (LED) and a spectrophotometer (as the detector) that operates in the visible range.

2. Methods and materials

2.1. Reagents and materials

Gold(III)Chloride solution, ~ 30 wt. % in dilute HCl, 99.99% (Catalogue No. 484385), also known as Tetrachloroaurate (HAuCl_4), was obtained from Aldrich. Aminosilane (*N*-[3-trimethoxy silyl] propyl) ethylenediamine, $>99\%$, also known as Aminopropyl trimethoxy silane (APTMS), was obtained from Aldrich. Trisodium citrate dehydrate was purchased from Merck Ltd. and acetic acid was purchased from SD Fine chemicals, India. SU8 and its developers were obtained from Microchem, USA. All the reagents were of analytical grade. All solutions were prepared using de-ionized (DI) water obtained from a MilliQ filtration system.

2.2. Design and fabrication

In our previous paper, we have discussed the fabrication of integrated U-bend waveguides with microchannels for evanescent wave absorption based detection.³ SU-8 was patterned as a U-bend waveguide and microchannel network in a single step fabrication scheme. In this study, we have used the same micro

^aDepartment of Biosciences and Bioengineering, IIT Bombay, Mumbai, 400076, India. E-mail: mukherji@iitb.ac.in; Fax: +91 22 25723480; Tel: +91 22 25767767

^bCentre for Research in Nanotechnology and Science, IIT Bombay, Mumbai, 400076, India

^cCentre of Excellence for Nanoelectronics, IIT Bombay, Mumbai, 400076, India

† Electronic supplementary information (ESI) available: Fig. S1–S3. See DOI: 10.1039/c005253a

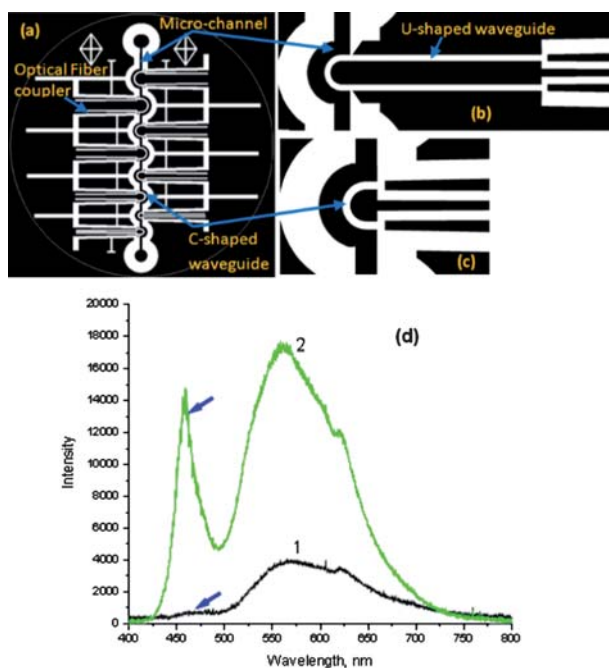


Fig. 1 (a) Showing the present Mask design of the device comprising of a network of microchannel and C-shaped waveguides with optical fiber coupler structure. (b) Showing a closer look at the previously reported Mask design explaining the microchannel interfacing with the long legged U-shaped waveguide.⁸ (c) Showing a closer look at the present Mask designs explaining the microchannel interfacing with the C-shaped waveguide coupled with the microchannel. (d) Intensity vs. Wavelength graph across (1) U-bend and (2) C-bend waveguides. The blue arrow indicates an enhancement of the transmission at peak wavelength 455 nm. The SU8 absorbs much of the energy in these wavelengths.

fabrication scheme for making waveguides coupled with the microchannel network, however, to enhance inherent transmission losses in those sections of the waveguide, which behave as light guides only and have no role in sensing, we retained only the curved portion of the U-bend waveguide and reduced the length of the input and output arms of the waveguide. As a result, the structure becomes C-shaped as opposed to U-shaped.

A modification in mask design was made to achieve this (Fig. 1a and c). We were able to get a 5 to 10 fold increase in the overall transmittance using C-shaped waveguides as compared to U-bend waveguides (Fig. 1d). It shows an overall improvement in transmission including at peak wavelengths of 455 nm, 560 nm and 625 nm.

The fabrication procedure is similar to our earlier study,³ however after fabrication of the structures, the surface of SU-8 was functionalized using aminosilane prior to immobilization of gold nanoparticles, as explained in a subsequent section.

2.3 SU-8 Silanization

The crosslinked SU-8 surface usually have large numbers of epoxy groups as compared to few –OH groups (which can bind to the silane monomer). According to the earlier literature, the remaining terminal epoxy groups in the cross-linked polymer can be converted into terminal –OH groups by hydrolysis using a strong acid or alkali.¹⁶ However, it is likely, and it was observed

that, prolonged exposure (more than 10–15 s) to strong acids or bases may damage the micro featured waveguides, creating cracks on the surface which modified the optical properties and caused channel leakage. To avoid this damage we used dilute 3% acetic acid in silane solution itself to make the silane solution pH \sim 3. This mild acid treatment along with silane solution for 5 min created enough –OH groups on the SU8 surface on which the APTMS molecule attached to form a uniform aminosilane layer on the surface. According to the earlier reports, pH at this level also helps in the orientation of the amine groups of APTMS away from the SU8 surface so that GNP can bind electrostatically to the amine group.¹⁷

2.4 Liquid phase Silanisation

The silane solution was prepared by adding 2% (w/v) APTMS to a mixture of ethanol and water (95 : 5). 3% acetic acid was added to adjust the pH of the solution to approximately 3. This solution was injected into the micro-channel and kept for 5 min. Then the channel was flushed with ethanol for 4 min to remove extra silane followed by a DI water flush for another 2 min. The channel was purged with dry air to remove the DI water inside the channel. Afterwards, the silanised surface was kept for 24 h at room temperature for condensation of the silane layer and to make this layer stable.

2.5 Synthesis of gold nanoparticles

Gold nanoparticles of \sim 23 nm size (Fig. 2a,b) used in these experiments were synthesized by the procedure described by Turkevich *et al.*¹⁸

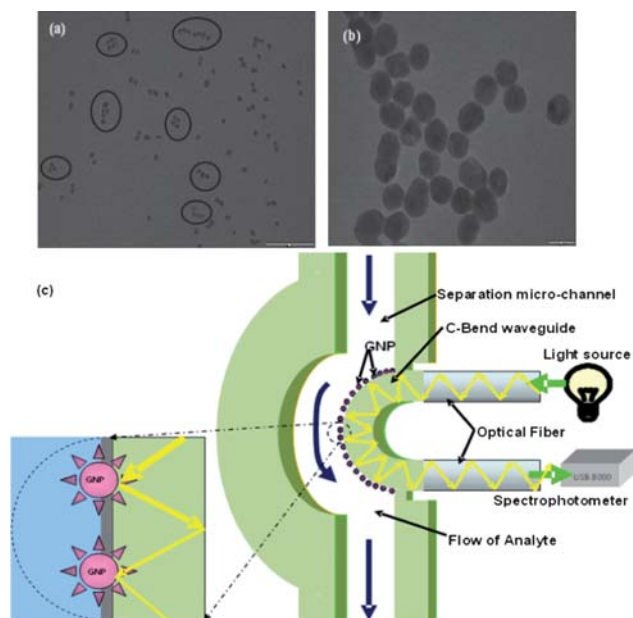


Fig. 2 (a) Showing the TEM images of the gold nanoparticles synthesized, scale bar: 200 nm (b) Showing a closer look at the GNP synthesized in aggregate form, scale bar: 20 nm. Encircled area indicates gold nanoparticle aggregates. (c) Schematic of optical set-up and sensing scheme used for experiments with the GNP-coated, C-bent SU8 waveguide coupled microchannel.

2.6 Immobilisation of gold nanoparticles over waveguide

Immobilisation of GNP over silanised C-shaped waveguides was done by simply filling the silanised microchannel with the GNP suspension and incubating for 1 h at room temperature (Fig. 2c). After 1 h, the gold nanoparticle suspension was flushed out using DI water and finally the channel was purged with dry air.

2.7. Optical set-up

The optical set-up for absorbance measurements (as explained diagrammatically in Fig. 2c) consisted of a white light emitting diode (Edison Opto, Taiwan, Model No. EDSW-1LAS-B1 of 10 Lumen intensity and 1 watt power with spectral emission between 430 and 700 nm) and a fiber optic spectrometer (Ocean Optics Model, USB 4000). One of the ends of the waveguide was coupled to a polished end of the optical fiber (core diameter: 200 μm) through fiber coupler structure. The other polished end of this prepared fiber was held by a fiber chuck in fiber coupler (Newport[®], USA). A microscopic objective lens, 40X, 0.6 NA was used to focus light from white LED onto the fiber end. The other end of the waveguide was similarly coupled to the fiber optic spectrometer through an intermediate 200 μm optical fiber. The absorbance spectra was obtained continuously during the experiments using Spectrasuite[®] software. The absorbance changes over time for a particular wavelength was calculated from the acquired data. Signal-to-noise (SNR) was improved by averaging 50 consecutive spectra.

3. Results and discussions

3.1. Formation of GNP SAMs on SU8 waveguide

Absorbance of light at 530 nm across C-shaped waveguide was monitored during the GNP immobilisation procedure using Spectrophotometer. At the point of introduction of GNP solution in to microchannel a sudden increase in absorbance at 530 nm was observed as shown in Fig. 3. The absorbance reached nearly 0.108 units within a short time span of only 2 s of

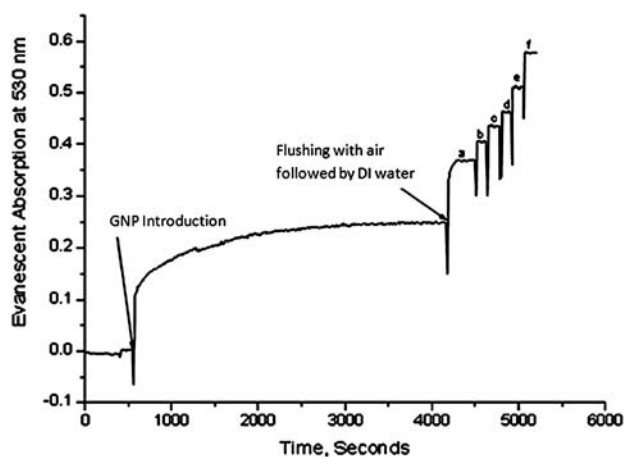


Fig. 3 Real time changes in absorbance recorded during GNP coating on C-bent waveguide of 1 mm bend radius and onwards introduction of various RI solution in the microchannel. (a)1.33299, (b)1.33587, (c)1.34026, (d)1.34477, (e)1.35096, (f)1.36889.

incubation, after which the rate of rise was relatively slow. The shape of the curve indicates an approximately first order response with a short time constant, which can be expected, given the relative dimension of the microchannel and the reaction. After 1 h of incubation, the waveguide probes were flushed once with air and then with DI water. The absorbance goes down steeply when the channel is filled with air. Absorbance increases up to 0.37 units after this flushing with DI water. This may be attributed to traces of GNP from upstream parts of the system getting desorbed from the surfaces and reaching the C-Bend to get adsorbed on the surface. So to ensure that such an event does not occur again during the actual testing phase, the channel was flushed for 2 to 3 min with DI water until the absorbance reading stabilises at one point. Finally the channel was filled with DI water.

3.2. Absorbance sensitivity to refractive index changes

Testing of the analyte solution refractive index sensitivity of GNP coated C-bent SU8 probes were performed previously as a continuous experiment after real time GNP adsorption on silanized SU8 waveguide. Here after the complete GNP immobilisation, sucrose solutions of different concentrations with refractive index between 1.33 and 1.37 were introduced and real time absorbance at 530 nm was recorded. A significant rise in absorbance was obtained with rising RI of different sucrose solutions (Fig. 3 a, b, c, d, e, f).

The same GNP coated waveguide was used in a separate experiment for refractive index sensitivity. The evanescent absorbance at GNP coated waveguide interfacing the DI water was taken as background signal. The evanescent absorbance of

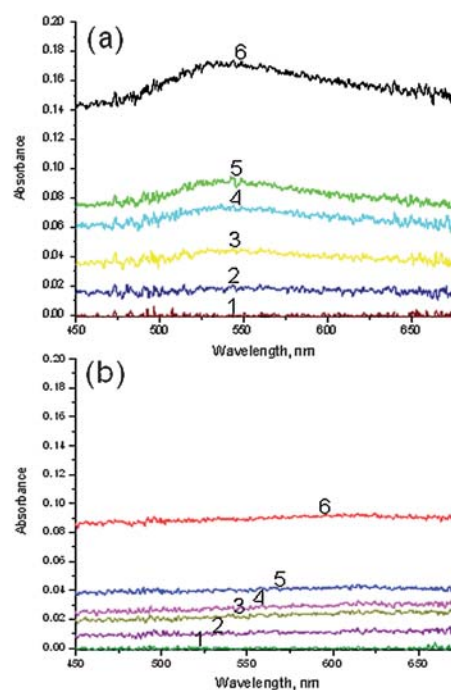


Fig. 4 Evanescent absorbance spectra of same dimension (a) GNP coated SU8 waveguide and (b) bare SU8 waveguide at refractive indices (1)1.33299, (2)1.33587, (3)1.34026, (4)1.34477, (5)1.35096, and (6)1.36889.

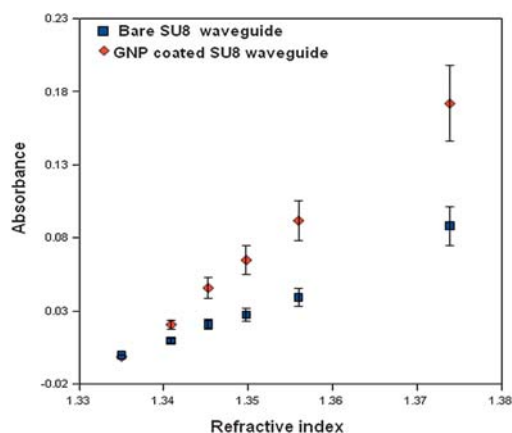


Fig. 5 Calibration curve for refractive index changes using varied concentrations of sucrose.

various higher RI solutions from 1.33 to 1.37 was observed with respect to the same background. The Fig. 4a confirms that an absorbance peak of 530 nm becomes more prominent when the channel was filled with higher refractive index sucrose solution. For comparative analysis the same experiment was repeated with same dimension bare SU8 waveguide probe (without GNP coating) and the absorption spectrum is shown in Fig. 4b. A flat spectral response, as expected, is seen in this case. The absorbance values for the bare and GNP coated waveguides at 530 nm for different refractive indices are plotted in Fig. 5. It can be clearly seen that the sensitivity to variation in refractive indices in the micro-environment is twice in case of the latter (GNP coated) waveguides. Sensitivity, defined as the ratio of the change in absorbance to the change in RI, was found to be relatively linear between 1.33 and 1.37 RIU and of value approximately $5 A_{530\text{nm}}/\text{RIU}$ for the probe.

4. Conclusion

Our earlier report had demonstrated the fabrication and efficacy of U-bend embedded polymer waveguides, where the waveguide formed part of the wall of a microfluidic channel. It was noticed that the cross sectional dimension of the waveguide and the native absorption in the polymer, leads to a low light output, which in turn affects the signal-to-noise ratio. In this study, improvements were made to waveguide design, so that the light travels through a shorter distance in the polymer. This significantly improved the light output and thereby has the potential to improve the SNR. A further improvement to the sensitivity of these waveguides to changes in refractive index variations in the micro-environment were brought about by developing a protocol to immobilize gold nanoparticles on the waveguide surface. As a result, the sensitivity increased to twice that of bare SU-8 waveguides of similar size and shape. It was observed, however, that the doubling of sensitivity is far less than that reported by Sai *et al.*,¹⁵ who used optical fibre waveguides. This may be to do with the fact that in this case, the active area (interfacing with the

microchannel) comprises of only one side of the waveguide and is about two tenths of the waveguide surface. Further, the active area in the probe used by Sai *et al.* was $\sim 12 \text{ mm}^2$ as compared to 0.2669 mm^2 ($A = 0.17 \times 3.14 \times 0.5$) area of the C-bend SU8 waveguide.

As in the case of the earlier design, the microfabrication process used is a single step and it can be mass fabricated easily. As in all evanescent absorption based sensors, the colour or optical density of the analyte solution does not make a significant difference unless the dye molecules or other molecules get adsorbed on the surface of the waveguide. Adding the GNPs to the surface of the waveguide also enhances the possibility that the output will show comparatively higher sensitivity to larger molecules bound to the surface of the GNPs.

5. Acknowledgements

This research was supported by grants from Centre of Excellence for Nanoelectronics, IIT Bombay. We thank SPM facilities Physics Department for AFM studies, sophisticated Analytical Instrument Facility (SAIF), IIT Bombay, for TEM images acquired and XRF studies in support of this study. Amit Prabhakar thanks VVR Sai for his help.

6. References

- 1 K. B. Mogensen, N. J. Petersen, J. Hubner and J. P. Kutter, *Electrophoresis*, 2001, **22**, 3930–3938.
- 2 J. Hubner, K. B. Morgensen, A. M. Jorgensen, P. Friis, P. Telleman and J. P. Kutter, *Rev. Sci. Instrum.*, 2001, **72**, 229–233.
- 3 Amit Prabhakar and Soumyo Mukherji, *Lab Chip*, 2010, **10**, 748.
- 4 P. K. Jain, X. Huang, I. H. El-Sayed and M. A. El-Sayed, *Plasmonics*, 2007, **2**(3), 107–118.
- 5 P. Englebienne, *Analyst*, 1998, **123**, 1599–1603.
- 6 K. C. Grabar, R. G. Freeman, M. B. Hommer and M. J. Natan, *Anal. Chem.*, 1995, **67**, 735–743.
- 7 T. Okamoto, I. Yamaguchi and T. Kobayashi, *Opt. Lett.*, 2000, **25**, 372–374.
- 8 N. Nath and A. Chilkoti, *Anal. Chem.*, 2002, **74**, 504–509.
- 9 H.-Y. Lin, C.-T. Chen and Y.-C. Chen, *Anal. Chem.*, 2006, **78**, 6873–6878.
- 10 F. Frederix, J.-M. Friedt, K.-H. Choi, W. Laureyn, A. Campitelli, D. Mondelaers, G. Maes and G. Borghs, *Anal. Chem.*, 2003, **75**, 6894–6900.
- 11 Jonathan C. Riboh, Amanda J. Haes, Adam D. McFarland, Chanda Ranjit Yonzon and Richard P. Van Duyne, *J. Phys. Chem. B*, 2003, **107**, 1772–1780.
- 12 Amanda J. Haes, Lei Chang, William L. Klein and Richard P. Van Duyne, *J. Am. Chem. Soc.*, 2005, **127**, 2264–2271.
- 13 L.-K. Chau, Y.-F. Lin, S.-F. Cheng and T.-J. Lin, *Sens. Actuators, B*, 2006, **113**, 100–105.
- 14 A. Leung, P. M. Shankar and R. Mutharasan, *Sens. Actuators, B*, 2008, **131**(2), 640–645.
- 15 V. V. R. Sai, Tapanendu Kundu and Soumyo Mukherji, *Biosens. Bioelectron.*, 2009, **24**, 2804–2809.
- 16 E. P. Plueddemann (1982), *Silane coupling agent*, Plenum Press, New York.
- 17 B. Arkles, J. Steinmetz and J. Hogan, Polymeric Silane Coupling Agents Enhance Strength of Composites, *Modern Plastics*, 1987, **64**(4), 138.
- 18 J. Turkevich, P. C. Stevenson and J. Hiller, *Discuss. Faraday Soc.*, 1951, **11**, 55–75.